NACA RM E52A11

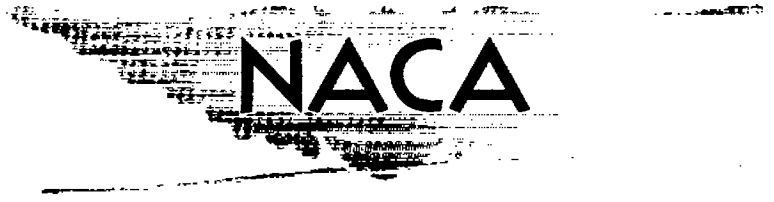

RESEARCH MEMORANDUM

ANALYSIS OF A PNEUMATIC PROBE FOR MEASURING EXHAUST-GAS TEMPERATURES WITH SOME PRELIMINARY EXPERIMENTAL RESULTS

By Marvin D. Scadron

Lewis Flight Propulsion Laboratory
Cleveland, Ohio

NATIONAL ADVISORY COMMITTEE
FOR AERONAUTICS

WASHINGTON
May 21, 1952

NATIONAL ADVISORY COMMITTEE FOR AERONAUTICS

RESEARCH MEMORANDUM

ANALYSIS OF A PNEUMATIC PROBE FOR MEASURING EXHAUST-GAS TEMPERATURES WITH SOME PRELIMINARY EXPERIMENTAL RESULTS

By Marvin D. Scadron

SUMMARY

A pneumatic probe based on continuity of mass flow through two restrictions separated by a cooling chamber was constructed to measure gas temperature at and beyond the limit of thermocouples. This probe consisted of a subsonic flat-plate orifice for the first restriction and a sonic-flow converging-diverging nozzle for the second restriction. The effect of variation in gas constants on the calibration is examined for common engine-exhaust gases. A high-temperature wind tunnel that allowed calibration of the probe at temperatures up to 2000° R and Mach numbers up to 0.8 is described. Agreement to better than 30° R between pneumatic probe indication and the indication of a rake of radiation-shielded thermocouples indicates that extrapolation of the calibration to higher temperatures is possible with fair accuracy.

INTRODUCTION

Measurement of gas temperatures is a basic requirement in evaluating the performance of a jet or gas-turbine power plant. Unless the relations between the pressure, velocity, and temperature distribution profiles are reliably known and the pressures and velocities can be measured with sufficient accuracy at a given cross section, a point-by-point traverse measurement of temperature is necessary in order to determine the temperature distribution profile. The most common method of making such measurements is to insert a thermocouple at the point at which the measurement is desired. This procedure is generally acceptable when the gas temperature at the point of measurement is not so high as to weaken the structure of the thermocouple probe or to affect the temperature-emf relation of the thermocouple wire. With the advent of engines of the ram-jet type and of engines using afterburners, higher gas temperatures than those readily measurable with thermocouples are attained and considerable difficulty is encountered in the measurement of these gas temperatures.

For the range of point-temperature measurements beyond that readily obtained with thermocouples, the pneumatic probe method appears to be applicable. The method consists of equating the mass flow rate at two points in a probe as obtained by metering devices at these points. The hot gas passes through the first metering device (usually an orifice or nozzle), is cooled to a temperature that can be measured with small error, and then passes through the second metering device. By proper arrangement of the mass flow equations, the gas temperature in front of the first metering device can be derived explicitly.

A method employing this principle, described in reference 1, consists of a probe with two subsonic flat-plate orifices in series, the first orifice being located in the hot gas at the point where the measurement is desired. The use of two restrictions in series eliminates the need for the knowledge of the mass flow rate of gas and permits the expression of the hot gas temperature in terms of measured gas pressure ratios and a cooled-gas temperature. In reference 2, a method is described where the time for a known quantity of gas to pass through an orifice is measured to provide an indication of the gas temperature in front of the orifice. A variation of the design described in reference 1 is presented in reference 3, wherein two sonic-flow flat-plate orifices in series are used. A comprehensive bibliography on the subject of pneumatic probes appears in reference 4. For certain point-temperature measurement applications, which required ease of use and a wide temperature range, a third variation of the pneumatic probe described in reference 1 (utilizing a subsonic flat-plate orifice as the first restriction and a sonic converging-diverging nozzle as the second restriction) met the requirements most conveniently. Some results obtained with this pneumatic probe at the NACA Lewis laboratory are presented herein.

Among the problems that occur in the application of pneumatic probes to the measurement of high gas temperature are: the variation of the coefficient of discharge of the restrictions with mass-flow rate, the measurement of temperature at the second restriction, change or variation of the gas constituents as they influence the calibration constants of the instrument, and the establishment of the range of temperature over which accurate measurements are obtainable. These effects are analyzed in detail in this report. Acquirement of means for testing and evaluating any actual instrument also presents a serious problem. At the Lewis laboratory a high-temperature wind tunnel, providing temperatures up to 2000° R, was available for calibration purposes. A suitable thermocouple system was installed in this wind tunnel to provide a standard of comparison with measurements made by a pneumatic probe inserted in the wind tunnel test section. Although these tests were made at a maximum temperature of about 2000° R, the reasonable agreement obtained between pneumatic probe indications and thermocouple indications suggests that the probe is applicable for use at higher temperatures such as those encountered in afterburners or in ram jets.

NOMENCLATURE

The following symbols are used in this report:

A	area
C_D	discharge coefficient
g	acceleration of gravity
H	total pressure
K	instrumental constant
M	Mach number

p static pressure

R specific gas constant

T total temperature

W mass flow

Y $\gamma_1/(\gamma_1-1)\left[(p_3/H_1)^{2/\gamma_1} - (p_3/H_1)^{(\gamma_1+1)/\gamma_1}\right]$

γ ratio of specific heats

$F(\gamma_1)$ $\gamma_1/(\gamma_1-1)$

$G(\gamma_4)$ $\dfrac{\sqrt{\gamma_4}}{\left(\dfrac{\gamma_4+1}{2}\right)^{\frac{\gamma_4+1}{2(\gamma_4-1)}}}$

Subscripts:

1 conditions immediately ahead of first restriction

2 conditions at throat of first restriction

3 conditions immediately behind first restriction

4 conditions immediately ahead of second restriction

5 conditions at throat of second restriction

6 conditions immediately behind second restriction

THEORETICAL ANALYSIS

A schematic drawing of the probe whose performance was investigated is presented in figure 1. By use of a vacuum pump or, in some cases, by use of ram pressure, a small portion of the hot gas is sampled by the probe and passed through two successive restrictions which are connected by a cooling chamber. The first restriction is designed to produce flow rates in the subsonic region only; the second restriction is a sonic-flow nozzle. Temperatures and pressures are measured in the vicinity of the second restriction at the stations indicated. Pressures only are

measured in the vicinity of the first restriction. The preceding symbols with subscripts relating the quantities to the stations indicated in figure 1 are used to express the mass-flow equations through a flat-plate orifice and through a sonic-flow nozzle:

$$W = C_{D,2}A_2H_1\sqrt{\frac{2g}{RT_1}\left(\frac{\gamma_1}{\gamma_1-1}\right)\left[\left(\frac{p_3}{H_1}\right)^{2/\gamma_1} - \left(\frac{p_3}{H_1}\right)^{(\gamma_1+1)/\gamma_1}\right]} \qquad (1)$$

for a flat-plate orifice, and

$$W = C_{D,5}A_5H_4\sqrt{\frac{g}{RT_4}}\frac{\sqrt{\gamma_4}}{\left(\frac{\gamma_4+1}{2}\right)^{(\gamma_4+1)/2(\gamma_4-1)}} \qquad (2)$$

for a sonic-flow nozzle. Equating the weight flows through the two restrictions permits solution for the temperature ratio:

$$\frac{T_1}{T_4} = 2\left(\frac{A_2C_{D,2}}{A_5C_{D,5}}\right)^2\left(\frac{H_1}{H_4}\right)^2\frac{F(\gamma_1)}{\left[G(\gamma_4)\right]^2}\left[\left(\frac{p_3}{H_1}\right)^{2/\gamma_1} - \left(\frac{p_3}{H_1}\right)^{(\gamma_1+1)/\gamma_1}\right] \qquad (3)$$

This equation is valid if the gases follow the general gas law and if the processes through the restrictions are isentropic. The temperature in front of the flat-plate orifice can be computed from measurements of the pressures at each restriction and of the temperature in front of the sonic-flow nozzle. The utility of equation (3) as a means of measuring the unknown gas temperature will depend on the extent to which the various quantities appearing in that equation may be treated as instrumental constants that vary negligibly with changing, and possibly unknown, gas conditions. Consideration will therefore be given to the effect on various terms in equation (3) of the gas temperature and of the specific heat ratios γ_1 and γ_4.

In order that the nature of the quantities T_1 and T_4 should be firmly established, the instrument was designed so that the measured and computed quantities would represent the total temperatures of the gas. The velocity of the gases immediately in front of each restriction were kept low by the use of small restrictions, large connecting tubes, and low mass-flow rates.

The effective area ratio term

$$\left[(A_2C_{D,2})/(A_5C_{D,5})\right]^2$$

can be made constant if the pneumatic probe is designed to operate at a proper mass-flow rate. Since the ratio of the orifice areas is fixed, any change in the effective area ratio term will be caused by a variation in the discharge coefficients $C_{D,2}$ and $C_{D,5}$. The discharge coefficient of a flat-plate orifice has been shown to be a function of the mass-flow rate (reference 5). The coefficient is zero at zero mass-flow rate. As the mass-flow rate increases, the discharge coefficient also increases until, at a certain flow rate, depending on the diameter ratio and the fluid characteristics, the coefficient stops increasing and becomes constant until the mass-flow rate reaches a value corresponding to sonic velocity at the orifice. Thereafter the discharge coefficient again increases with further increase in mass-flow rate, although sonic velocity persists at the throat of the orifice (reference 6). Consequently, the discharge coefficient at the flat-plate orifice can be maintained most nearly constant by maintaining a mass-flow rate slightly below that required to maintain sonic velocity at the throat of the orifice.

For the second restriction a converging-diverging nozzle, rather than a flat-plate orifice, was selected because the discharge coefficient of a nozzle is close to unity over a wide range of mass-flow rate, even when sonic flow exists at the throat of the nozzle. A nozzle was not chosen for the first restriction because of the very large temperature difference between the gas and the restriction and the larger heat-transfer surface of a nozzle compared with a flat-plate orifice. It could be conceivable that, by using a nozzle for the first restriction, sufficient heat could be transferred from the gas to the nozzle so that the assumption of an isentropic process through the nozzle would not be realized.

The specific heat ratios of the exhaust gas will vary with gas composition, which is a function of fuel-air ratio, temperature, and type of fuel used. The present analysis will be confined to hydrocarbon fuels having a hydrogen-carbon ratio ranging between 0.10 and 0.22. For the range of temperature expected, the specific heat ratio γ_1 at the first orifice can vary from 1.26 to 1.37, as shown in figure 4 of reference 7. The instrument was designed to cool the gas to about 700° R at the second restriction; at this temperature the specific heat ratio γ_4 upstream of the sonic-flow nozzle can vary from 1.36 to 1.40. The effects of the above variations in the value of γ_1 on the quantity

$$Y = F(\gamma_1)\left[\left(\frac{p_3}{H_1}\right)^{2/\gamma_1} - \left(\frac{p_3}{H_1}\right)^{(\gamma_1+1)/\gamma_1}\right]$$

average about 1 percent and exceed 2 percent in only a few cases. The value Y is tabulated in table I. The effect of variation of γ_4 over the range indicated on the quantity $\left[G(\gamma_4)\right]^2$ averages about ±1.0 percent. The value $\left[G(\gamma_4)\right]^2$ is tabulated in table II. The value $G(\gamma_4)$ was obtained from figure 8 of reference 7.

Consequently, equation (3) can be rewritten in the form

$$T_1/T_4 = K\,(H_1/H_4)^2\,Y \qquad (4)$$

where K is a constant equal to

$$2\left[(A_2C_{D,2})/(A_5C_{D,5})\right]^2 / \left[G(\gamma_4)\right]^2$$

and has a probable variation of 1.0 percent, and Y, if assumed known at an average value of γ_1 of 1.31, can be treated as a function solely of the pressure ratio p_3/H_1 with a probable variation of 1.1 percent. Equation (4) and table I thus provide a simple means for determining the unknown temperature T_1 in terms of the measured quantities T_4, H_1, p_3, and H_4.

CONSTRUCTION AND CALIBRATION OF PNEUMATIC PROBE

A scale drawing of the pneumatic probe is shown in figure 2. It resembles a pitot tube and its essential elements are a flat-plate orifice at the leading edge of the tube, a converging-diverging sonic-flow nozzle, a cooling-water jacket between the two restrictions, a thermocouple in front of the sonic-flow nozzle, and pressure taps and connecting tubing. The temperature upstream of the sonic-flow nozzle is measured with a 36 gage silver-shielded iron-constantan thermocouple of National Bureau of Standards design. Data on this design, appearing in reference 8, indicate a probable error in temperature T_4 of the order of 0.5 percent. Cooling water enters the probe through a tube that is directed at the first orifice plate and then passes along the outer shell of the protecting tube and is discharged outside the gas stream. The total pressure in front of the first orifice plate is measured by

stopping the flow, so that the instrument becomes a total-pressure tube with a pressure being measured by means of pressure tap H_1 or p_3. The temperature of the thermocouple upstream of the sonic-flow nozzle is measured with a manually balanced potentiometer having a sensibility of 0.1° F. Gas is sucked through the instrument by a positive displacement pump capable of maintaining a pressure of 4 inches of mercury absolute downstream of the diverging portion of the sonic-flow nozzle. The mass-flow rate is controlled by a 1/8-inch V-port control valve. The connections of the manometers used to measure the pressure drop across the restrictions, as well as absolute pressures, are shown in figure 3.

The effective area of each orifice was determined by passing room air through the instrument and measuring the flow rate accurately with a wet-type gas displacement meter. Pressure drops and temperatures at each restriction were measured. Inserting these measurements into equations (1) and (2) yielded the effective areas of the restrictions. The effective areas are plotted in figure 4 as functions of the pressure ratio. The pressure ratio shown in figure 4(b) represents the ratio between pressures at the extreme ends of the converging-diverging nozzle. The pressure at the throat of the nozzle was always equal to the value associated with sonic flow.

The square of the effective area ratio as it appears in the constant K of equation (4) can be obtained directly by means of the calibration just described. The temperature ratio is unity and therefore the area ratio term can be determined from equation (3). The value of this term is plotted in figure 5 as a function of pressure ratio across the flat-plate orifice.

In obtaining the effective area ratios, the square of the total-pressure ratio $(H_1/H_4)^2$ was also evaluated. The difference between H_1 and H_4 is a function of H_1-p_3 and of the upstream pressure H_1. The ratio $(H_1/H_4)^2$ is plotted against $(H_1-p_3)/H_1$ in figure 6. The average scatter of points is about 0.5 percent and the maximum deviation, about 1.2 percent.

From figure 5, the square of the effective area ratio term is approximately 5.36; from figure 6, the square of the total-pressure ratio is approximately 1.25; with an average value of $\gamma_4 = 1.38$ assumed from table II, a corresponding value of $\left[G(\gamma_4)\right]^2$ is equal to 0.465. Substitution of these values into equation (3) yields

$$T_1 = 28.9\ Y\ T_4 \qquad (5)$$

This equation is plotted in figure 7 with lines of constant T_4. The equation yields a maximum error of about 1.5 percent if γ_1 is known but γ_4 and $(H_1/H_4)^2$ are unknown. If γ_1 is unknown but an average value of 1.31 is assumed, an additional error of about 0.4 percent is obtained at high values of p_3/H_1 and an error of about 2 percent, at low values of p_3/H_1.

The data shown in figure 4 can be used to establish the temperature range of the pneumatic probe. The maximum pressure ratio at the first orifice is 0.96; for $\gamma_1 = 1.40$ the corresponding value of Y is 0.0383. The minimum pressure ratio of 0.60 corresponds to a value of Y of 0.228. The range of the temperature ratio that can be measured is given approximately by

$$\frac{(T_1/T_4)_a}{(T_1/T_4)_b} = \frac{0.228}{0.0383} = 5.96$$

where a and b indicate the extremes of the range, since the variation in temperature ratio is represented primarily by variations in the value of Y. If T_4 is held at 700° R, the maximum temperature T_1 which the pneumatic probe can measure is approximately 4200° R.

EXPERIMENTAL EVALUATION

The performance of the pneumatic probe was tested in a high-temperature wind tunnel over the following range of variations in gas conditions:

Variable	Range
γ_1	1.31 to 1.37
γ_4	1.38 to 1.39
H_1, in. Hg abs.	30 to 35
T_1, °R	1150, 1950, 2050
M	0.3 to 0.8

No effort was made to completely separate the effects of each variable. The wind tunnel was operated at one of the three temperature levels listed, and the free-stream Mach number was varied over the complete range given.

A schematic drawing of the high-temperature wind tunnel is shown in figure 8. Air for combustion was available at pressures up to 40 pounds per square inch gage and at mass flows up to 1000 pounds per minute. The fuel was 60 octane clear gasoline with a hydrogen-carbon ratio of 0.178. The fuel system supplied up to 100 pounds per minute of fuel to 8 spray nozzles at station A. After leaving the test section the products of the combustion were exhausted to the atmosphere through a muffler. The test-section diameter is 6 inches.

The temperature of the gas in the stagnation chamber, station B (fig. 8), was measured by a rake of platinum-shielded thermocouples following the National Bureau of Standards design described in reference 8. These thermocouples indicated gas temperature to a probable accuracy of 1/2 percent. Additional chromel-alumel thermocouples were attached to the walls of the stagnation chamber and to the test section at station C. Temperatures indicated by the thermocouples were read with a self-balancing potentiometer connected to the thermocouples through a selector switch. Figure 9 shows the location and the identification number of the major thermocouples in the stagnation chamber and the test section. A high recovery thermocouple (described in reference 9) was placed in the center of the test section to determine the change in total temperature of the gas stream between the stagnation chamber and the test section. This thermocouple is listed as number 19 on figure 9.

A total-pressure survey rake was installed at station B. Static-pressure taps were located in the test section wall at intervals of 1 inch. Pressures were read on a common-well, multiple-tube mercury manometer.

Fuel-flow rate was measured with a calibrated rotameter. A continuously indicating mixture analyzer sampled exhaust gas at station B.

During the operation of the tunnel some of the exhaust gas was passed between the inner walls of the stagnation chamber in order to heat the walls to gas temperature. A test run was made only after thermocouples peened into the walls indicated that the test-section wall was within 100° R of the total temperature of the gas.

With the burners shown, gas temperatures of about 2000° R were available at the entrance of the test section. Temperature and pressure surveys of the stagnation chamber were made at various operating conditions; typical results are shown in figures 10 and 11.

The variation in temperature across the stagnation chamber was less than 3 percent of the average temperature. Wall temperatures were usually within 4 percent of the average gas temperature. The difference between the high recovery thermocouple in the test section and the average of the 10 thermocouples in the stagnation chamber was never more than 12° R as shown in table III.

There was no measurable pressure gradient across the stagnation chamber. A total-pressure survey of the test section is shown in figure 12 and indicates that there was negligible total-pressure loss between the stagnation chamber and the test section to within 1 inch from the wall of the test section.

RESULTS AND DISCUSSION

A summary of the pneumatic probe data appears in table IV. The temperatures indicated by the pneumatic probe were calculated from equation (5). The maximum difference between the pneumatic probe and the average of ten thermocouples in the stagnation chamber was 28° R. Analysis of the data showed that the value of γ_1 was close to the average value chosen for use in equation (5). The pneumatic probe temperatures were also computed from equation (3) and the results were compared with the temperatures computed from equation (5). The values of temperature T_1 from these two equations agreed to within 0.3 percent.

Comparison of the pneumatic probe indications with the average of the thermocouples indicated that the greatest error appears at the lower Mach numbers and at the higher temperatures. This was probably a result of stagnation chamber thermocouple errors, which would be greatest under these conditions.

These preliminary results suggest that this method should be further investigated, with specific emphasis placed upon the following items:

(1) Proximity to an isentropic process of the flow through the first orifice

(2) The temperature and pressure range to which the general gas law can be considered applicable

(3) The degree to which the first orifice area remains constant with temperature increase and time

(4) The effect of pulsating flow, of the type found in ram jets and afterburners, on the accuracy of the calculated temperature

The preliminary data presented in this paper indicate that the probe may be used at higher temperature levels, provided suitable means of comparison are available.

SUMMARY OF RESULTS

A pneumatic probe was constructed using a flat-plate orifice and a sonic-flow nozzle. The probe was tested in a high-temperature wind tunnel where the gas temperature and gas velocity could be varied up to 2000° R and Mach number of 0.8, respectively. The probe was compared with a rake of ten platinum-shielded thermocouples with a maximum difference between the probe and the average of the thermocouples of 28° R. The preliminary results indicated that gas temperatures at higher levels may be measured, provided the general gas law is applicable.

Lewis Flight Propulsion Laboratory
National Advisory Committee for Aeronautics
Cleveland, Ohio

REFERENCES

1. Schmick, Hans: Über die Bestimmung von Gastemperaturen mittels Druckdifferenzmessung. Zeitschr. f. techn. Physik, Heft 10, Nr. 4, 1929, S. 146-147.

2. Cassan, M. H.: Pyromètre-Densimètre à gaz. J. des Usines a Gaz. vol. 53, 1929, pp. 527-532.

3. Blackshear, Perry L., Jr.: Sonic-Flow-Orifice Temperature Probe for High-Gas-Temperature Measurements. NACA TN 2167, 1950.

4. Freeze, Paul D.: Bibliography on the Measurement of Gas Temperatures. Circular 513, Nat. Bur. Standards, Aug. 20, 1951.

5. Rouse, Hunter: Fluid Mechanics for Hydraulic Engineers. McGraw-Hill Book Co., Inc., 1938, p. 260.

6. Perry, J. A., Jr.: Critical Flow Through Sharp-Edged Orifices. Trans. A.S.M.E., vol. 71, Oct. 1949, pp. 757-764.

7. Pinkel, Benjamin, and Turner, L. Richard: Thermodynamic Data for the Computation of the Performance of Exhaust-Gas Turbines. NACA ARR 4B25, 1944.

8. Fiock, Ernest F., and Dahl, Andrew I.: Final Report Summarizing Progress on the Development of Thermocouple Pyrometers for Gas Turbines. Nat. Bur. Standards, Jan. 31, 1951.

9. Scadron, Marvin D., Gettelman, Clarence C., and Pack, George J.: Performance of Three High-Recovery-Factor Thermocouple Probes for Room-Temperature Operation. NACA RM E50I29, 1950.

TABLE I - VALUES OF Y WITH VARYING PRESSURE RATIO AND RATIOS OF SPECIFIC HEAT

$$Y = \frac{\gamma_1}{(\gamma_1-1)}\left[\left(\frac{p_3}{H_1}\right)^{2/\gamma_1} - \left(\frac{p_3}{H_1}\right)^{(\gamma_1+1)/\gamma_1}\right]$$

p_3/H_1	γ_1			p_3/H_1	γ_1		
	1.26	1.31	1.37		1.26	1.31	1.37
0.995	0.00533	0.00507	0.00481	0.795	0.156	0.157	0.159
.990	.0102	.0101	.00962	.790	.158	.159	.161
.985	.0145	.0147	.0148	.785	.161	.162	.164
.980	.0194	.0194	.0192	.780	.163	.164	.167
.975	.0242	.0240	.0240	.775	.166	.167	.170
.970	.0291	.0291	.0288	.770	.168	.169	.172
.965	.0334	.0338	.0337	.765	.171	.171	.174
.960	.0383	.0380	.0381	.760	.173	.174	.177
.955	.0426	.0426	.0429	.755	.175	.176	.179
.950	.0470	.0473	.0474	.750	.177	.178	.181
.945	.0512	.0511	.0514	.745	.179	.180	.184
.940	.0562	.0553	.0559	.740	.181	.183	.186
.935	.0601	.0600	.0603	.735	.183	.185	.188
.930	.0645	.0642	.0648	.730	.185	.186	.190
.925	.0683	.0684	.0688	.725	.187	.188	.192
.920	.0727	.0722	.0729	.720	.189	.191	.194
.915	.0766	.0769	.0770	.715	.190	.192	.196
.910	.0809	.0807	.0811	.710	.192	.194	.198
.905	.0848	.0845	.0851	.705	.194	.196	.200
.900	.0882	.0883	.0888	.700	.196	.198	.202
.895	.0926	.0921	.0929	.695	.197	.199	.203
.890	.0960	.0959	.0966	.690	.198	.200	.205
.885	.0998	.0997	.100	.685	.200	.202	.207
.880	.103	.103	.104	.680	.201	.203	.208
.875	.107	.106	.108	.675	.202	.205	.210
.870	.111	.110	.111	.670	.204	.206	.211
.865	.114	.114	.115	.665	.205	.208	.212
.860	.117	.117	.118	.660	.206	.209	.214
.855	.121	.120	.122	.655	.207	.210	.215
.850	.124	.123	.125	.650	.208	.211	.217
.845	.127	.127	.128	.645	.209	.212	.218
.840	.130	.130	.132	.640	.210	.213	.218
.835	.133	.133	.135	.635	.211	.215	.220
.830	.136	.136	.138	.630	.212	.215	.221
.825	.140	.140	.141	.625	.213	.216	.222
.820	.142	.143	.144	.620	.213	.217	.222
.815	.145	.145	.147	.615	.214	.218	.224
.810	.148	.148	.150	.610	.215	.218	.224
.805	.151	.151	.153	.605	.215	.219	.225
.800	.153	.153	.156	.600	.216	.220	.226

TABLE II - COMPUTED VALUES OF $\left[G(\gamma_4)\right]^2$ FOR VARYING RATIOS OF SPECIFIC HEAT

$\left[G(\gamma_4)\right.$ obtained from reference 7$\left.\right]$

$$\left[G(\gamma_4)\right]^2 = \frac{\sqrt{\gamma_4}}{\left(\frac{\gamma_4+1}{2}\right)^{(\gamma_4+1)/2(\gamma_4-1)}}$$

γ_4	1.400	1.390	1.380	1.370	1.360	1.350
$\left[G(\gamma_4)\right]^2$	0.470	0.468	0.465	0.463	0.461	0.459

TABLE III - SAMPLE DATA

[Temperature distribution in stagnation chamber and total temperature change between stagnation chamber and test section]

Thermocouple	Temperature (°F)							
	Run							
	1	2	3	4	5	6	7	8
1	960	975	972	1175	1166	841	803	797
2	OUT	----	----	----	----	---	---	---
3	970	983	979	1182	1173	836	805	797
4	968	980	975	1180	1170	836	802	795
9	900	927	925	1107	1115	760	755	745
10	920	950	950	1129	1145	763	772	764
11	927	958	958	1135	1153	772	780	774
12	913	941	948	1120	1135	762	765	755
19	973	1010	1010	1183	1223	772	800	782
20	978	1012	1013	1186	1220	784	812	795
21	981	1015	1016	1187	1220	786	813	796
22	980	1015	1014	1186	1217	786	813	796
23	980	1014	1013	1185	1214	789	813	796
24	940	988	1003	1179	1207	786	809	795
25	976	1011	1010	1187	1220	781	806	790
26	976	1012	1010	1189	1224	783	806	791
27	976	1011	1008	1188	1220	782	806	791
28	971	1008	1003	1185	1213	781	805	790
29	968	1001	998	1180	1209	780	800	786
Average stagnation temperature	973	1009	1009	1179	1216	784	808	793
Test-section Mach number	0.794	0.601	0.402	0.655	0.460	0.753	0.552	0.352

TABLE IV - SUMMARY OF DATA
[Comparison of instrument with platinum-shielded thermocouples]

Run	Average thermocouple temperature ($^{\circ}R$)	Test section Mach number M	Ratio of specific heats γ_1	Pneumatic probe temperature ($^{\circ}R$)	Difference between pneumatic probe and thermocouple temperature ($^{\circ}R$)
1	1172	0.352	1.367	1181	9
2	1174	.399	1.365	1182	8
3	1170	.488	1.364	1174	4
4	1180	.601	1.364	1176	-4
5	1178	.678	1.363	1176	-2
6	1175	.794	1.363	1176	1
7	1458	.349	1.349	1480	22
8	1472	.402	1.347	1486	14
9	1468	.501	1.345	1486	18
10	1463	.655	1.343	1474	11
11	1460	.753	1.341	1471	11
12	1455	.794	1.339	1468	13
13	2080	.350	1.319	2108	28
14	2075	.399	1.318	2102	27
15	2068	.460	1.317	2088	20
16	2072	.601	1.315	2088	16
17	2067	.690	1.313	2082	15
18	2062	.790	1.311	2075	13

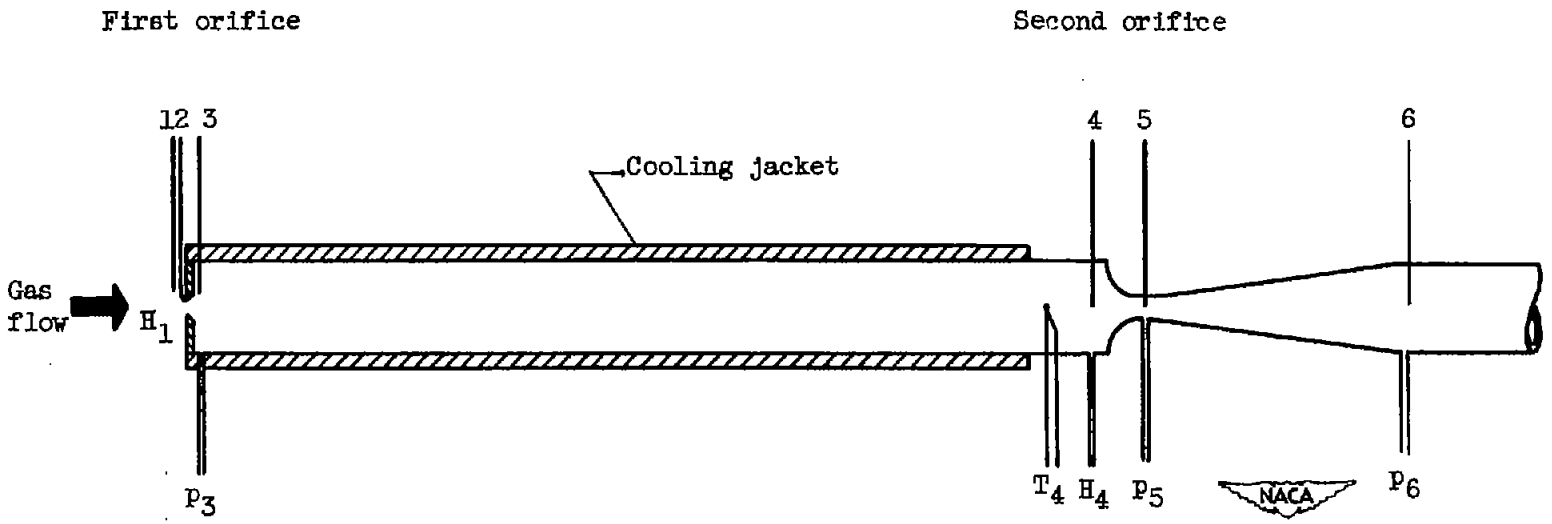

Figure 1. - Schematic drawing of instrument showing station locations.

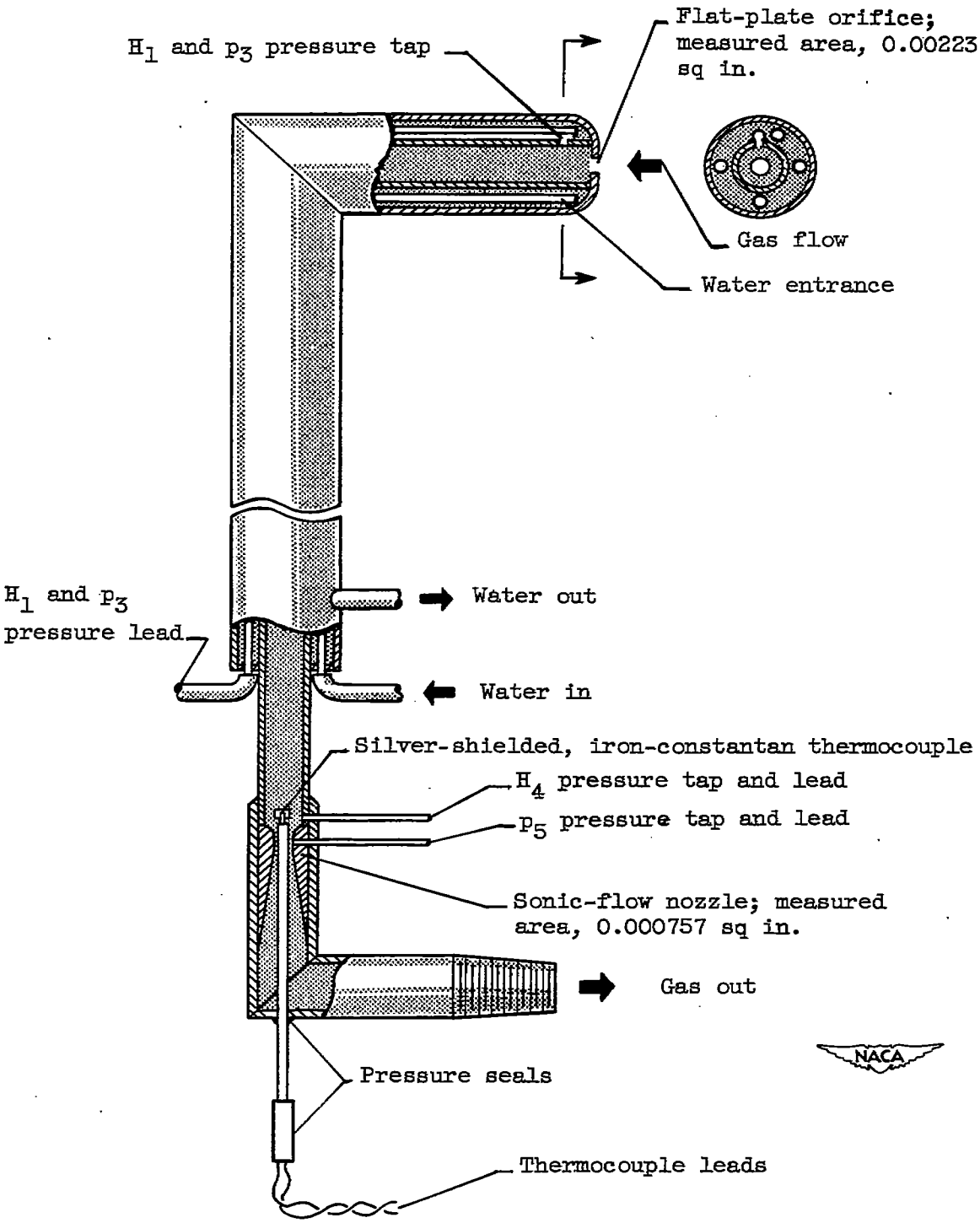

Figure 2. - Detail drawing of temperature measuring instrument under test.

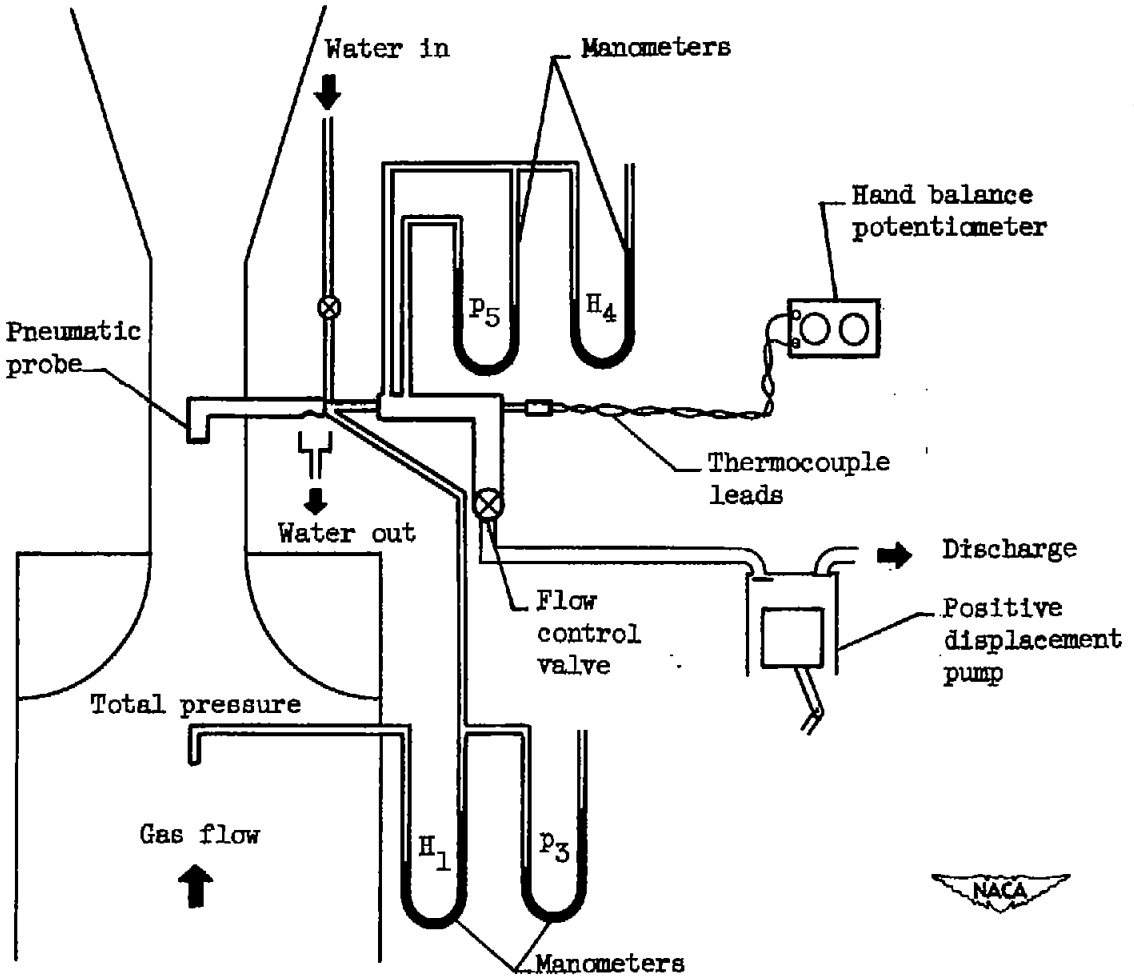

Figure 3. - Schematic drawing of method of testing temperature measuring instrument in high-temperature, high-velocity tunnel.

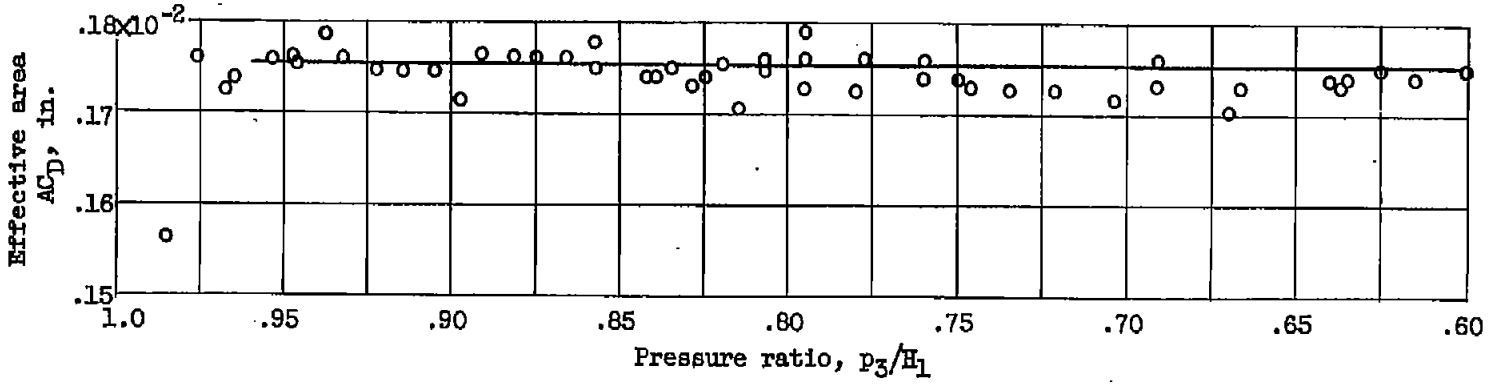

(a) First orifice.

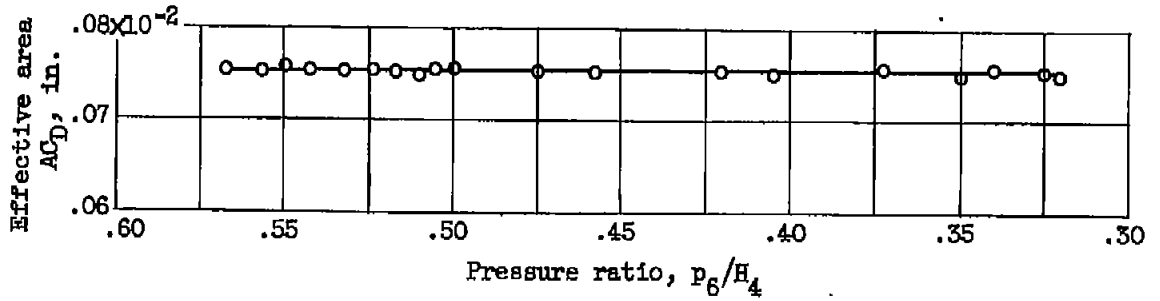

(b) Second orifice.

Figure 4. - Effective area as function of pressure ratio across orifice. H_1, atmospheric pressure.

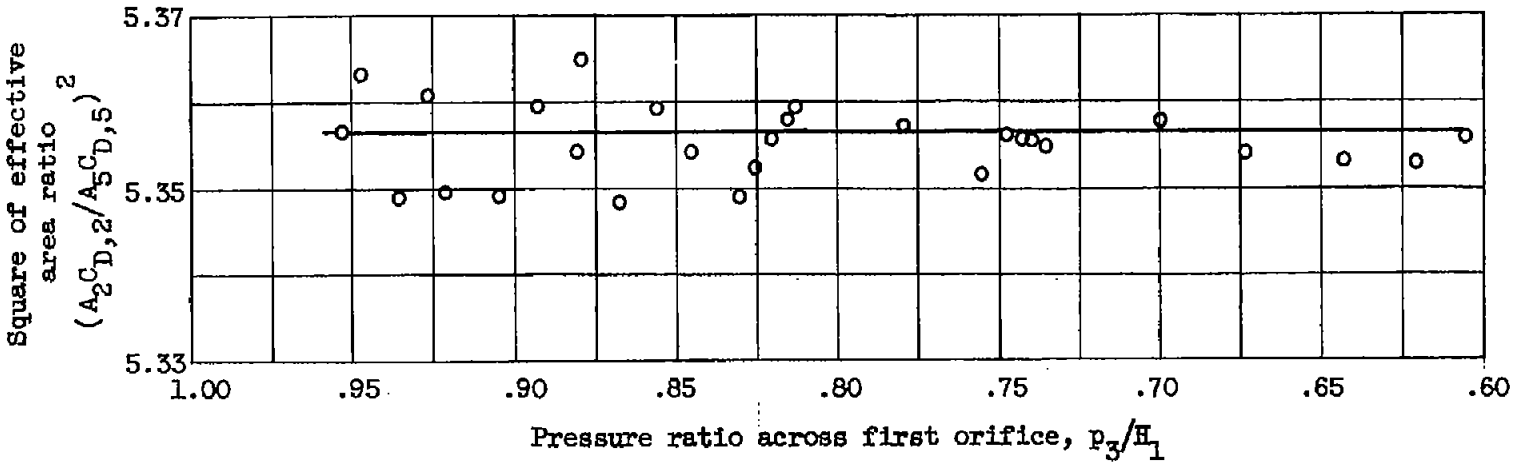

Figure 5. - Evaluation of area ratio term.

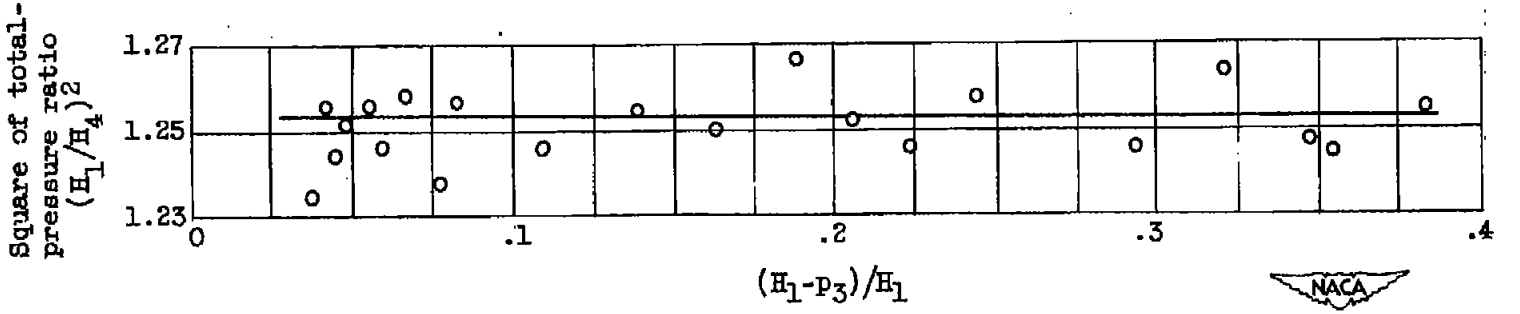

Figure 6. - Evaluation of pressure ratio term as function of pressure ratio across first orifice.

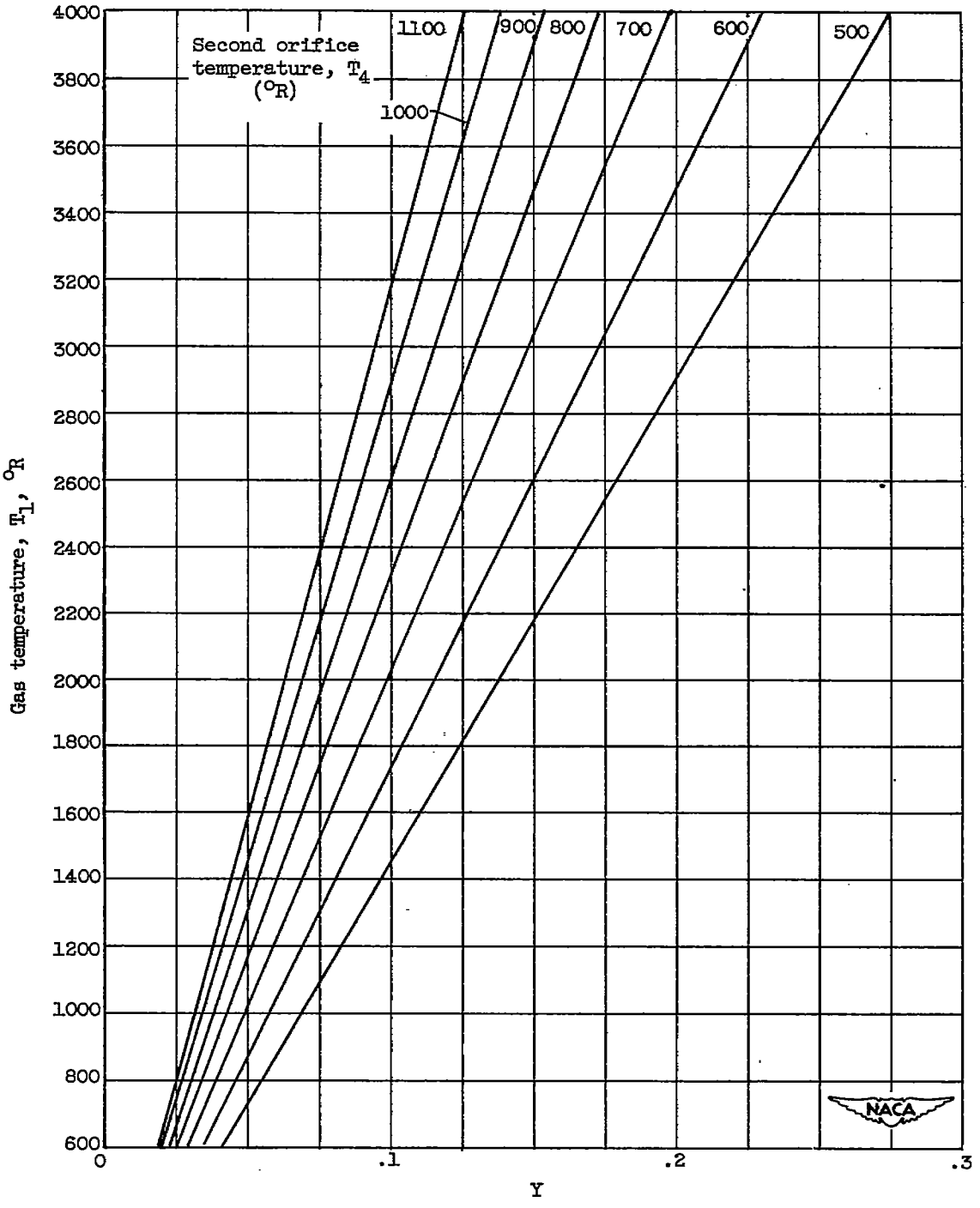

Figure 7. - Operating graph for temperature measuring instrument.

$T_1 = 28.9\ Y\ T_4$

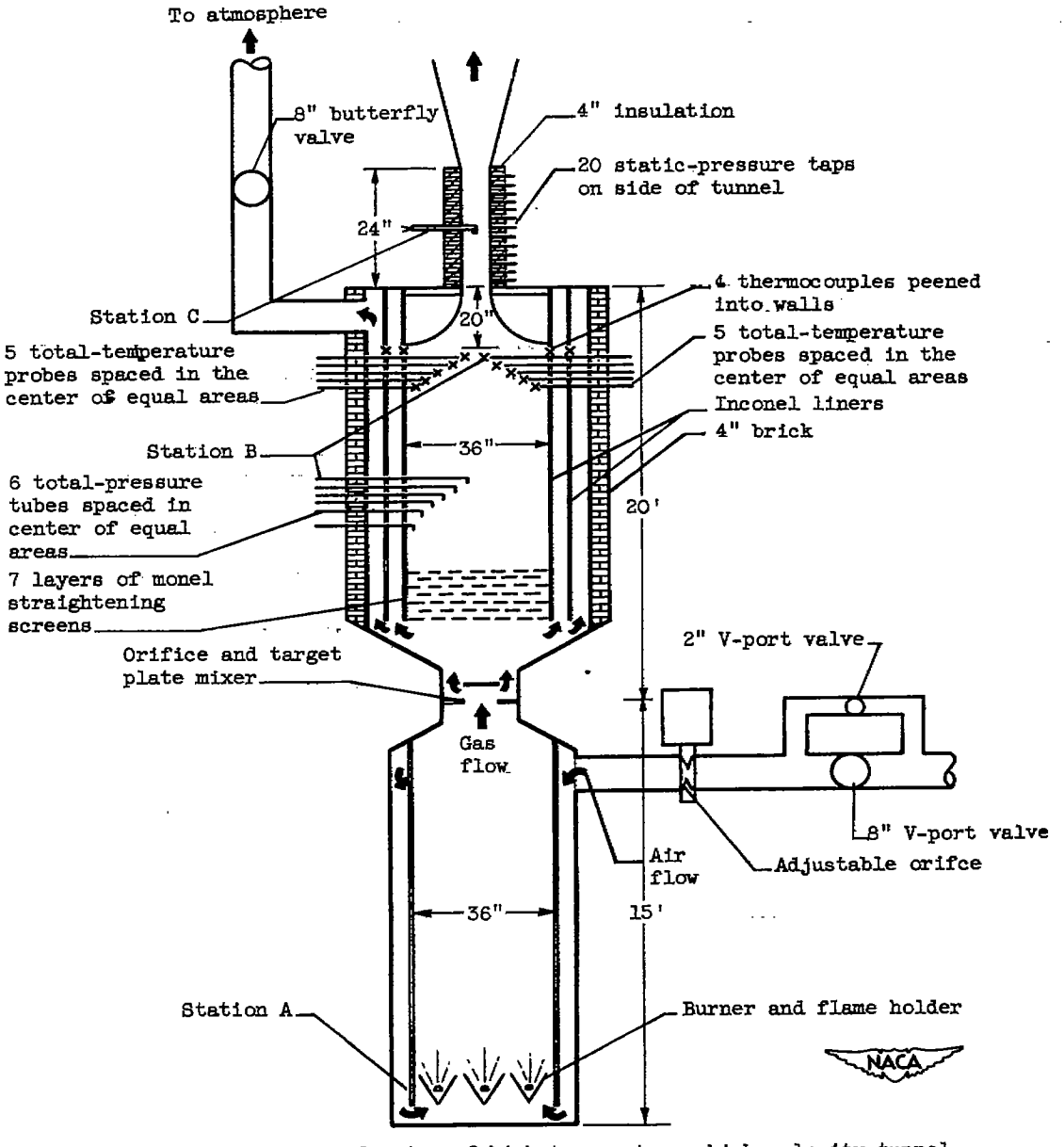

Figure 8. - Schematic drawing of high-temperature, high-velocity tunnel.

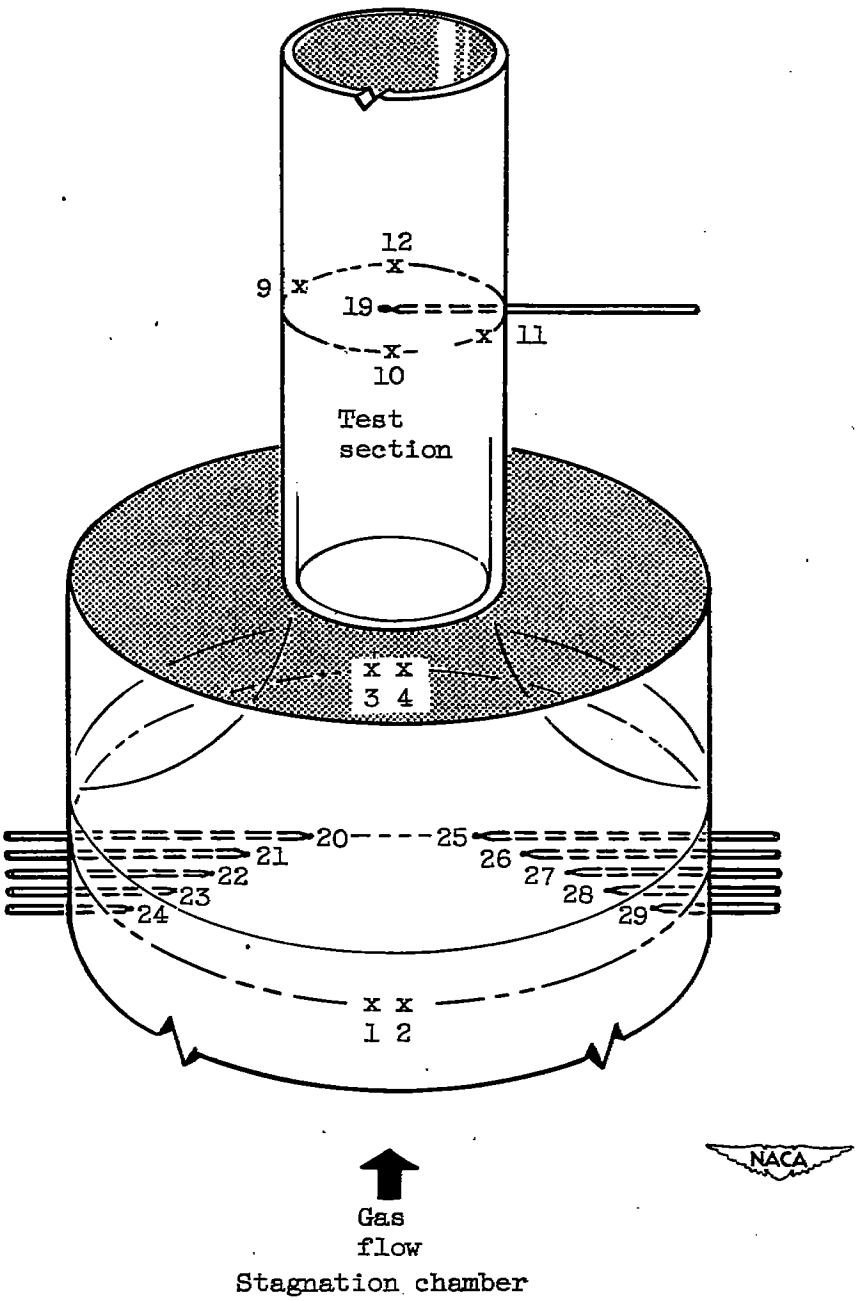

Figure 9. - Number and location of major thermocouples in stagnation chamber and test section to identify data appearing in table III.

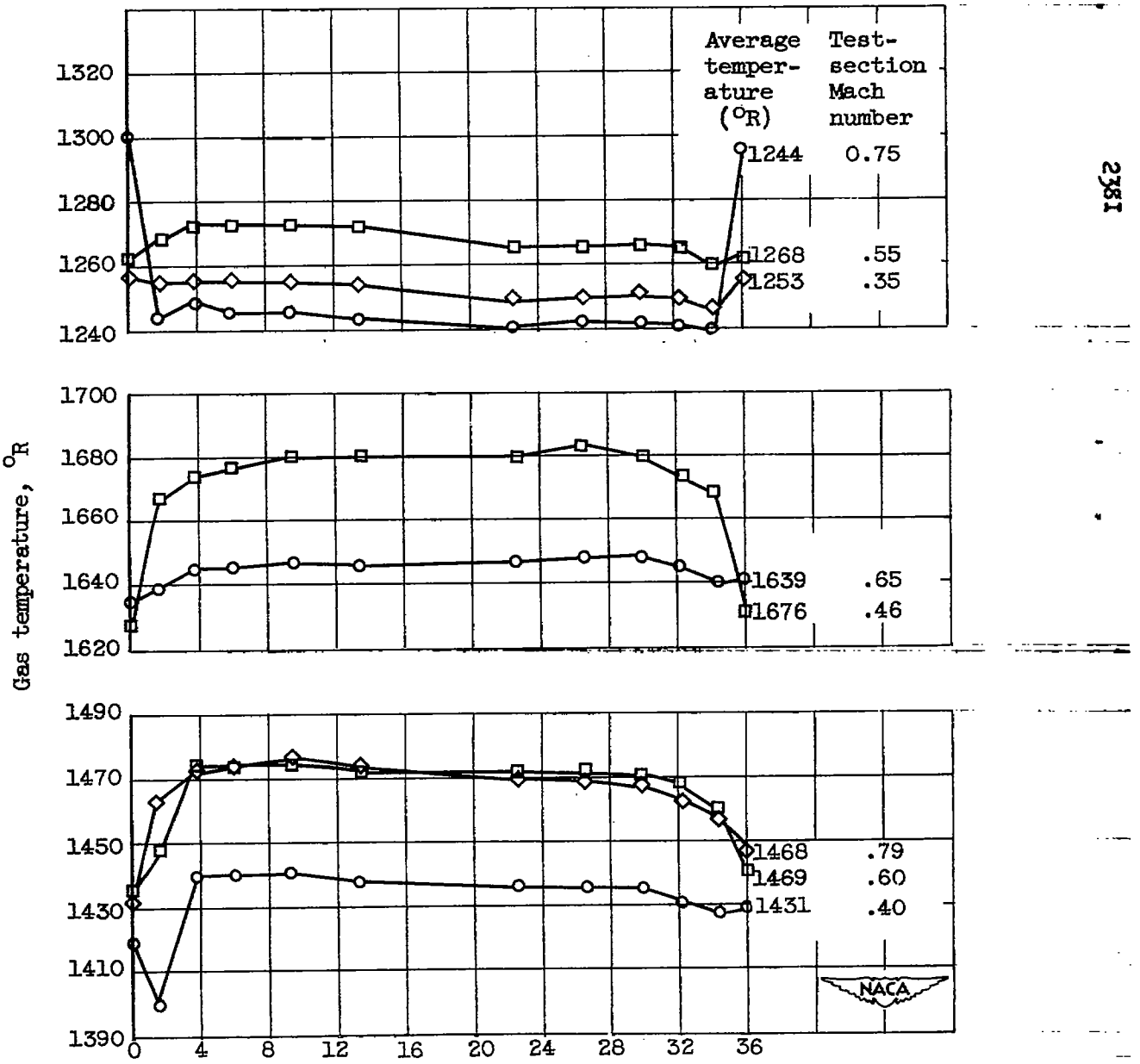

Figure 10. - Temperature distribution across stagnation chamber at station B.

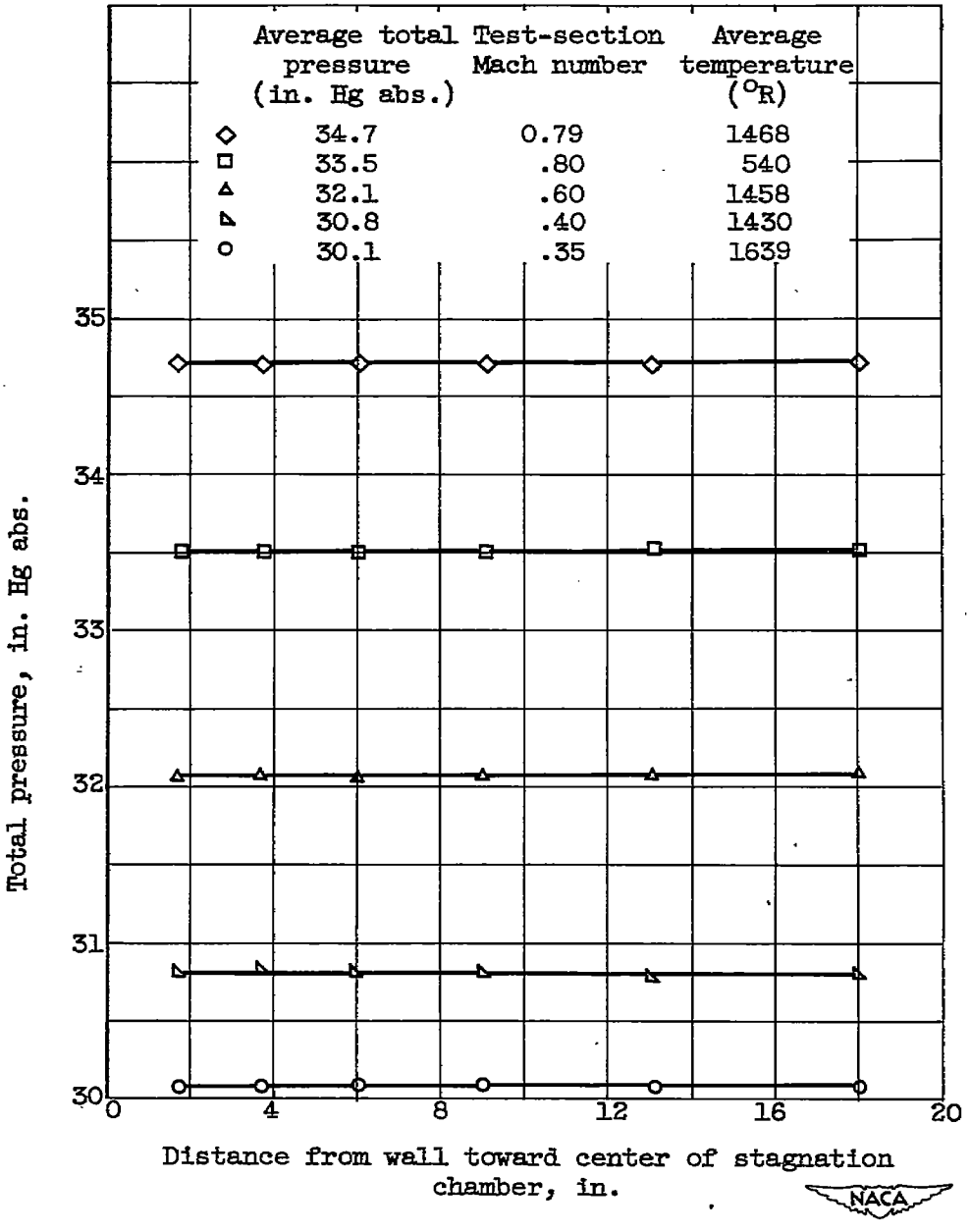

Figure 11. - Pressure distribution across half of stagnation chamber at station B.

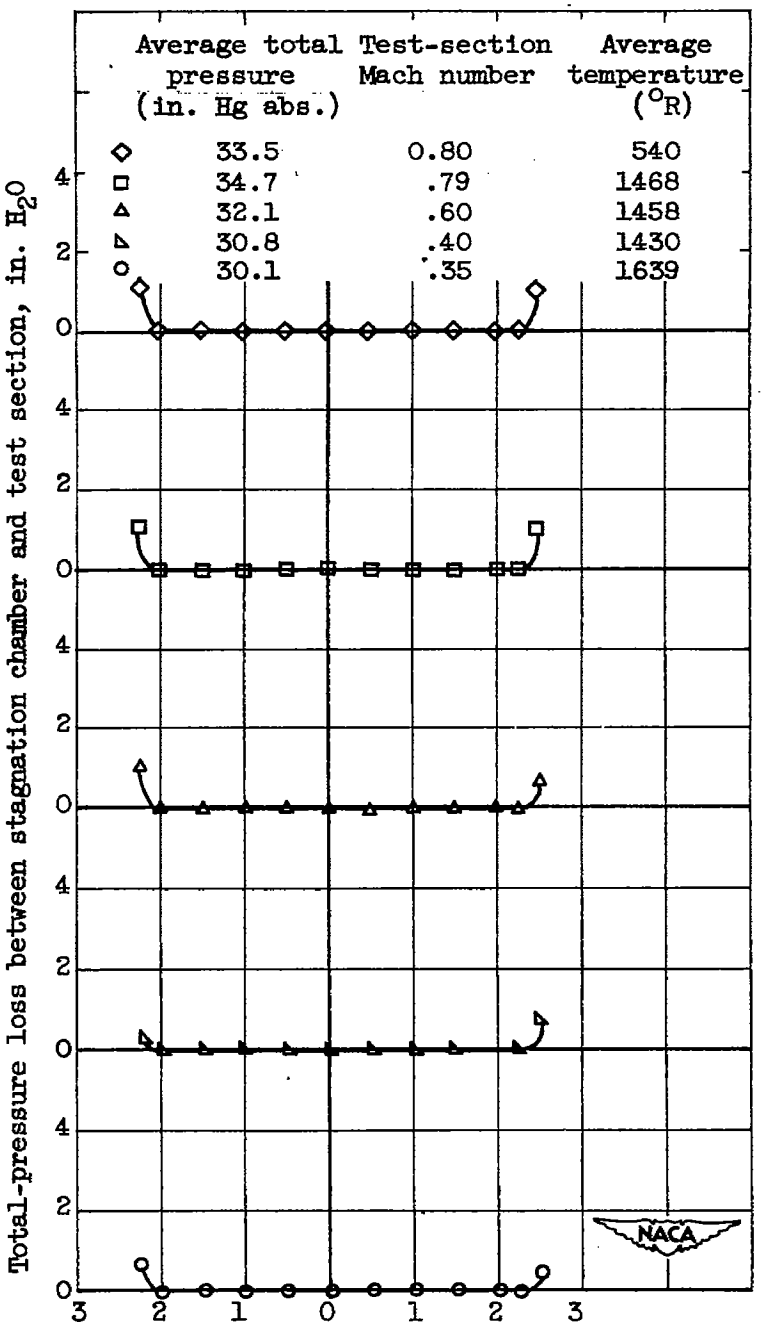

Figure 12. - Total-pressure distribution at station C and total-pressure loss between stations B and C.